Structure of the p-h nucleus ^{132}Sb

H. Mach, D. Jerrestam, B. Fogelberg, and M. Hellström*
Department of Neutron Research, Uppsala University, S-61182 Nyköping, Sweden

J. P. Omtvedt
Department of Chemistry, University of Oslo, P.O. Box 1033 Blindern, N-0315 Oslo, Norway

K. I. Erokhina
Ioffe Physicotechnical Institute, Russian Academy of Sciences, Politekhnicheskaya ul. 26, St. Petersburg, 194021 Russia

V. I. Isakov
St. Petersburg Nuclear Physics Institute, Russian Academy of Sciences, Gatchina, 188350 Russia
(Received 1 August 1994)

Spins and parities of the low-lying states in ^{132}Sb populated in the β^- decay of ^{132}Sn have been determined from conversion electron and $\gamma\gamma(\theta)$ studies. $B(M1)$ and $B(E2)$ transition rates were obtained for a number of transitions in ^{132}Sb using the $\delta(E2/M1)$ ratios deduced from the $\gamma\gamma(\theta)$ data and the level lifetimes measured with the fast timing $\beta\gamma\gamma(t)$ method. A close agreement between the experimental transition rates and those calculated with a quasiboson approximation model provides a strong confirmation of the theoretical scheme and the effective forces used in the calculations.

PACS number(s): 21.10.Tg, 23.20.Gq, 21.60.Cs, 27.60.+j

I. INTRODUCTION

The structure of nuclei at double shell closures is of considerable theoretical importance and motivates intensive experimental studies. The occurrence of doubly-magic regions is quite rare and for the medium-heavy nuclei (for $A > 56$) only the region near ^{208}Pb has been studied in some detail. The recently improved ion source [1] at the OSIRIS fission-product mass separator at Studsvik/Sweden allows studies of the ^{132}Sn region in greater detail. Consequently we have undertaken a comprehensive investigation of ^{132}Sn and of several nuclei in its close vicinity. Our new results on ^{132}Sb are summarized in the present paper.

The structure of ^{132}Sb provides a unique opportunity to study the coupling of a valence proton particle to a neutron hole outside the doubly magic ^{132}Sn core. At present, levels in this nucleus can be populated only in the β^- decay of ^{132}Sn, and due to the low spin of the parent state, $J^\pi = 0^+$, only a limited number of levels is populated in this decay. The first account of the level scheme of ^{132}Sb was given by Kerek *et al.* [2], while more detailed γ-ray singles and $\gamma\gamma(t)$ studies have been reported by Stone, Faller, and Walters [3]. A summary of the previous experimental results is given in Ref. [4]. On the theoretical side energy spectra, electromagnetic transition rates, and β-decay properties were recently calculated by Erokhina and Isakov [5] for the odd-odd nuclei close to the doubly magic ^{132}Sn, i.e., for ^{134}Sb, ^{130}In, ^{132}Sb, and ^{132}In, using a quasiboson approximation model. However, a critical verification of the model predictions requires more detailed experimental data, in particular measurements of absolute transition rates.

The present study, which includes measurements of conversion electron and $\gamma\gamma(\theta)$ angular correlations, as well as time-delayed $\beta\gamma(t)$ and fast timing $\beta\gamma\gamma(t)$ measurements, has clarified not only the spin/parity assignments to the levels in ^{132}Sb but also established absolute transition rates for a large number of transitions. Importantly, the new experimental data provide a critical verification of the model predictions by Erokhina and Isakov [5].

II. EXPERIMENTAL DETAILS

Measurements were performed at the OSIRIS fission-product mass separator [6]. The ion source, containing 1 g of ^{235}U, was operated in a surface ionization mode [1]. The $A = 132$ activities, which included short-lived ^{132}In ($T_{1/2}$=0.22 s) and ^{132}Sn ($T_{1/2}$=40 s), were isobarically separated from other products of the thermal-neutron induced fission of ^{235}U. The activities of interest were deposited onto an Al-coated Mylar tape, which was moved with a cycle time that minimized the contribution from competing long-lived isobars. Generally the decays of ^{132}In$\rightarrow^{132}$Sn and ^{132}Sn$\rightarrow^{132}$Sb were studied at the same time using a 5 s tape cycle. However, two measurements, time-delayed $\beta\gamma(t)$ and fast timing $\beta\gamma\gamma(t)$, were repeated with the aim to enhance the decay of ^{132}Sn to ^{132}Sb, in

*Present address: National Superconducting Cyclotron Laboratory, Michigan State University, East Lansing, MI 48824-1321.

TABLE I. Experimental and theoretical (Ref. [7]) K-conversion coefficients for γ rays in ^{132}Sb.

E_γ (keV)	α_K^{exp} Ref. [2]	α_K^{exp} This work	α_K^{th} $E1$	α_K^{th} $M1$	α_K^{th} $E2$	Multipolarity [a]	$\mid \delta(E2/M1) \mid$
85.6	0.83(8)		0.25	0.85	1.9	$M1(+E2)$	<0.25 [b]
246.9	0.046(9)	0.050(5)	0.0135	0.046	0.059	$M1(+E2)$	<1.1 [c]
340.5	0.021(4)	0.018(2)	0.0056	0.020	0.021	$M1/E2$	
899.0		0.0016(4)	0.00062	0.0019	0.0015	$M1/E2$	

[a]Notation: $M1(+E2)$ means that transition was found to be predominantly $M1$ with a possible admixture of $E2$ given by δ in column 8, while $M1/E2$ means that the multipolarity may be either $M1$ or $E2$ or $M1+E2$.
[b]A similar limit of $\mid \delta \mid \leq 0.25$ is obtained from the measured value of α_L=0.13(3) (Ref. [2]).
[c]Using the average value of α_K=0.049(4).

which case the tape was moved every 1 min. The results on the decay of ^{132}In$\rightarrow^{132}$Sn will be published separately. All measurements were performed at the point of beam deposition.

A. Conversion electrons

Conversion electrons were measured with a cooled 2 mm thick Si(Li) detector, which had an active area of about 100 mm^2. The Al-coated Mylar tape was placed at 45° to the incoming beam so the activity directly faced the Si(Li) detector. A small plastic scintillator, which served as β detector, was placed behind the tape, and a large volume Ge detector was placed opposite to the Si(Li) detector. Electron and γ-ray spectra were recorded simultaneously, both as ungated and β-gated spectra. The latter helped to reduce a continuous β background in the electron spectra. The α_K coefficients obtained in the present work and listed in Table I compare well with the previous results [2]. The 85.6- and 246.9-keV lines are identified as $M1$ transitions with a possible $E2$ admixtures for which upper limits are given in column 8. The 340.5- and 899.0-keV lines are identified as either $M1$, $E2$, or $M1+E2$. The result for the 899.0-keV line is quite important since it establishes a positive parity for the 426.1- and 85.6-keV levels as well as the ground state (g.s.), see Fig. 1.

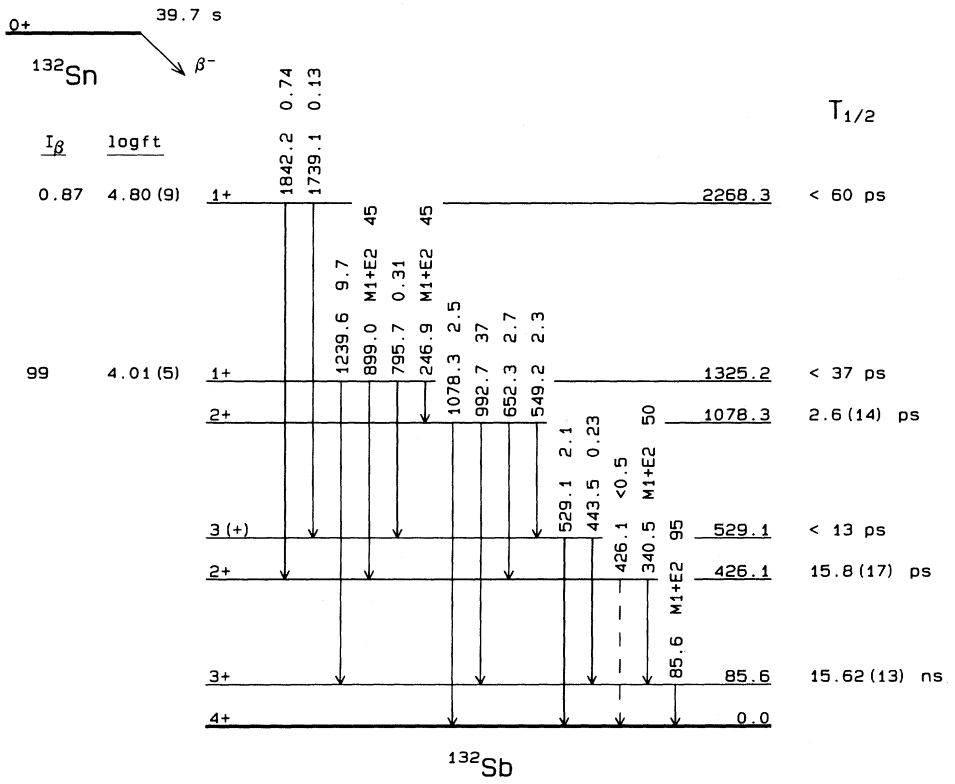

FIG. 1. Partial decay scheme of ^{132}Sn$\rightarrow^{132}$Sb (from Ref. [4]). Spin/parity assignments and level half-lives are from this work. Energy levels are not plotted according to scale.

TABLE II. Summary of the level lifetime determinations in ^{132}Sb.

Level Energy (keV)	$T_{1/2}$ previous [a] (ns)	$T_{1/2}$ this work [b] (ns)
85.6	14.8(18)	15.62(13) [c]
254.5	102(4) [d]	
426.1	$\leq$2	0.0158(17)
529.1		$\leq$0.013
1078.3	$\leq$2	0.0026(14)
1325.2	$\leq$0.8	$\leq$0.037
2268.3		$\leq$0.060

[a]From Ref. [2] unless stated otherwise.
[b]Averaged from $\beta\gamma\gamma$(t) measurements unless stated otherwise.
[c]The average includes $T_{1/2}$=15.63(20) ns from $\beta\gamma(t)$ measurement.
[d]From Ref. [9].

B. Time-delayed $\beta\gamma(t)$ measurements

A search was made for level lifetimes in the nanosecond range using a time-delayed coincidence set-up characterized by a time resolution of FWHM$\sim$12 ns at E_γ=100 keV that included a thin plastic scintillator as β detector and a small Ge detector for γ rays. The analysis of strong transitions in ^{132}Sb revealed a long lifetime only for the 85.6-keV line. Its lifetime obtained using a slope fitting technique [8] is included in Table II.

C. Fast timing measurements

Lifetimes in the picosecond range were measured using the $\beta\gamma\gamma(t)$ method detailed in Refs. [8,10,11]. Three independent measurements were performed (Run-I, Run-II, and Run-III) characterized by different electronics, calibration procedures, and tape cycle times. Each run was part of a self-contained series of timing measurements which included the decays of interest and those for the calibration purposes.

The triple coincidence set-up consisted of three detectors positioned in a plane around the beam deposition point. Lifetime information was deduced from time-delayed $\beta\gamma(t)$ coincidences in two fast timing detectors: a thin plastic scintillator for β rays (a 2 mm thick Pilot-U in Run-I, a 5 mm NE111A in Run-II, and a 3 mm thick NE111A in Run-III) and a conically shaped BaF_2 crystal (2.5 cm in height) for γ rays. An additional γ coincidence with a Ge detector served to select the desired decay path and to simplify the energy spectrum observed in the BaF_2 crystal. The plastic and BaF_2 scintillators were coupled to the fast photomultiplier tubes (XP2020 and XP2020Q in Run-I, and a pair of XP2020QUR in the later runs) operated in the anode mode [10]. A constant fraction unit ORTEC 584 used in Run-I was replaced by ORTEC 935 in Runs II and III. The overall time resolution was FWHM$\sim$200 ps at E_γ=1 MeV in Run-I and about 130 ps in the subsequent runs.

Data were collected in quadruplets ($E_\gamma^{BaF_2}, E_\beta, E_\gamma^{Ge}, \Delta t_{\rm fast}$) in Run-I, and in quintuplets in Runs II and III. As the fifth parameter, a time delay between feeding β transition and a deexciting γ ray in the "slow" Ge detector, $\Delta t_{\rm slow}$, was collected and used to subtract random events recorded in germanium. Timing spectra were sorted off-line with gates set on two full-energy peaks (and their respective backgrounds): one in germanium and one in BaF_2, respectively, while a common gate was set on the β spectrum [11]. Note that any timing distribution is uniquely defined by two numbers $[A, B]$, which stand for energies in keV of the transitions selected in germanium and BaF_2, respectively.

For energetic β rays a thin plastic scintillator acts as a ΔE β detector and provides a β response almost independent of the feeding β-ray energy, which plays a crucial role in the data analysis [8,11]. However, the decay of ^{132}Sn$\rightarrow^{132}$Sb has a low $\beta_{\rm max}$ energy of only $\sim$1.8 MeV. Nevertheless, since most of the β feeding (99%) goes to a single level at 1325.2 keV (see Fig. 1), the use of a common gate on the β spectrum yields results that are equivalent to the ΔE detector case. Small β branchings to other levels (below 1%) provide no interference in the data analysis.

With the exception of the 85.6-keV level (long lifetime) and the 1325.2-keV state (top level), all other lifetimes were measured by the centroid shift technique [8]. Here, the mean life τ ($\tau = T_{1/2}/\ln 2$) of a level directly β fed is given by the difference between the centroid of the delayed time spectrum and the prompt centroid of the same E_γ. When the level of interest is fed by a γ ray from a higher-lying level, the mean life of interest is given by the difference between the centroid shift of the spectrum gated by the deexciting γ ray and the centroid shift of the spectrum gated by the feeding γ transition.

The prompt and delayed time spectra must be measured concurrently in order to maintain identical conditions in the face of small but persistent drifts of the electronics. The calibration process involves "prompt points" or "reference points" which are internal to the decay and serve to renormalize the relative prompt curve (prompt positions as a function of γ-ray energy) measured separately [8,10,11].

In Run-I the relative prompt was obtained following a simple procedure [12] previously applied in Refs. [13,14], which consisted of a single run with the A = 96 beam, as the decay schemes of ^{96}Rb$\rightarrow^{96}$Sr and ^{96}Sr$\rightarrow^{96}$Y are simple and the lifetimes of several key levels in ^{96}Sr and ^{96}Y have recently been measured [12] with high precision. The resultant precision in the relative prompt determination was only $\sigma_\tau\approx$10 ps. In Runs II and III several calibration beams were used giving $\sigma_\tau\approx$2–3 ps.

As for the reference points, the decay of ^{132}Sn represents a special case. In the centroid shift analysis, if all the β feeding goes to one level (labeled "top level"), then its lifetime remains undetermined, unless it is long enough to be measured by fitting the slope. In other words, since within one decay all the centroid shifts are measured relative to the feeding γ ray, then for all the transitions in the decay there exists a "reference" feeding transition except for those deexciting the top level, for

which there exists none. Since the lifetime of the top level cannot be determined in the centroid shift analysis, its value becomes irrelevant and can be treated as $\tau=0$. Consequently, transitions deexciting this level provide reference points and may even define a relative prompt on their own. In the case of the 1325.2-keV level in ^{132}Sb (see Fig. 1), there are three deexciting transitions of energy 246.9, 899.0, and 1239.6 keV, which span a wider energy range than the transitions in this decay for which a prompt determination is needed. The relative prompt was thus renormalized to those three reference points.

In particular, the relative prompt curve was renormalized to the centroids of the [993,247], [340,899], and [86,1240] time spectra (where $[A,B]$ means energies in keV of transitions selected in germanium and BaF_2, respectively). These positions were confirmed by the centroids of the intense [86,899] and [86,247], as well as of the weaker [549,247], [652,247], and [1078,247] time distributions. The lifetimes of the 426.1- and 1078.3-keV levels were measured as differences between the relative prompt and the centroids of the [899,340] and [247,993] time distributions, respectively. A close confirmation of those lifetimes was obtained from the centroid shifts from the relative prompt of the [86,340] and [86,993] time spectra, respectively. The lifetime of the 529.1-keV state was obtained from the centroid shift of the [549,529] time spectrum from the relative prompt after subtraction of the mean life of the 1078.3-keV state (deduced above). The lifetime limit of the 2268.3-keV level was estimated from very weak [1842,340] and [86,1842] time distributions.

The lifetime of the 85.6-keV level was obtained from fitting the slope of the [993,86] time distributions (see Fig. 2). The same technique [8] was used to extract an upper limit of the lifetime of the 1325.2-keV state, since it was not possible to identify any slope due to the lifetime of the 1325.2-keV level neither in the [340,899] time distribution nor in any other time spectrum analyzed here. The lifetime results are summarized in Table II. The averaged values listed in column 3 supersede the preliminary results quoted in Refs. [15,16].

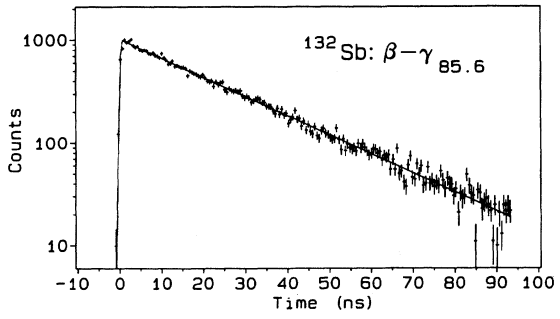

FIG. 2. Time-delayed spectrum between feeding β particles (start) and the 85.6-keV γ rays (stop) with an additional gate on the 899.0-keV γ transition in Ge. The lifetime of the 85.6-keV level is obtained from slope fitting (the fit is indicated by a solid line). An abrupt cutoff at 95 ns is caused by the 100 ns limit selected on the range of the Time-to-Amplitude-Converter.

D. Angular correlation measurements

The $\gamma\gamma(\theta)$ angular correlation set-up consisted of five Ge detectors arranged around the beam deposition spot at distances varying from 6.3 to 10.6 cm away from the source. In order to minimize the effects due to different detector efficiencies [which varied from 20% to 80% relative to the standard NaI(Tl) detector], the distance for each germanium was selected in such a way that all detectors exhibited similar counting rates.

The angles between various combinations of detector pairs, θ, were selected to provide the angular correlations with a maximal sensitivity at $\theta=0°$ and 90° and with some coverage for the angles in between. In order to define detector positions relative to the incoming beam, we use variables ϕ and φ, where ϕ is the angle in the horizontal plane, while φ is the angle relative to the horizontal plane. The Ge detectors were positioned at the angles $(\phi,\varphi)=(182°, 0°)$, $(270°, -30°)$, $(90°, 54°)$, $(60°, 0°)$, and $(240°, 0°)$, respectively. The error in the angle determination was typically less than 2°.

In the analysis, energy gates were set on the γ rays in ^{132}Sb, and the coincident spectra were sorted out for all unique combinations of detectors (20 possibilities). The peak areas corresponding to the observed coincidences between a pair of γ rays, E_1-E_2, were extracted from all the spectra with the pertinent background spectra subtracted. The analysis was performed separately for the γ-ray pairs E_1-E_2 and for its reciprocal E_2-E_1. A consistency check between those results ensured that no spurious background yields that would mainly come from the compton peaks, were present in the data sets. The solid angle corrections were obtained following the procedures in Ref. [17].

The data points were fitted to a standard angular correlation function [18] for a two γ-ray cascade $(I_1 \xrightarrow{\delta_1} I_2 \xrightarrow{\delta_2} I_3)$ with no alignment of the initial state and with the following free parameters: δ_1, δ_2, and the detector efficiencies, leaving thus at least nine degrees of freedom. (For the sign of the δ mixing ratio we use the convention of Krane, Steffen, and Wheeler [19].) In some cases both δ_1 and δ_2 were kept fixed giving a fit with eleven degrees of freedom. Occasionally an optional relative efficiency was fixed for each detector to the values measured off-line, which increased the number of degrees of freedom up to the maximum limit of 15. This latter procedure served to ensure that the fitted angular correlation function was not spurious with pertinent efficiencies vastly different from the measured values.

III. ANALYSIS OF ANGULAR CORRELATIONS

The angular correlation data require independent limitations of the transition multipolarities and δ mixing ratios. In other words, if the spins are not firmly established and both δ_1 and δ_2 mixing ratios are to be determined simultaneously, the fitted parameters usually remain undetermined. In the present case the experimental lifetimes provide limits on the $E2$ admixture to some of the $M1+E2$ transitions in ^{132}Sb based on the assump-

tion that the $B(E2)$ rates are less or equal to 7 Weisskopf units (W.u.). These limits, which are $|\delta(E2/M1)| \leq 0.20$, ≤ 0.20, and ≤ 0.65 for the 246.9-, 340.5-, and 529.1-keV transitions, respectively, were used in the analysis of angular correlations as discussed below. We take 7 W.u. as an arbitrary upper limit of the $B(E2)$ enhancement, since the $B(E2)$ rates are found to be low in the vicinity of doubly magic ^{132}Sn, and thus one expects similar rates for the low-lying states in ^{132}Sb. Indeed, the model calculations [5] predict low $B(E2)$ rates for those states — generally well below 4 W.u.

The relatively short level lifetimes rule out any significant admixture of $M3$ or $E3$ multipolarity to the observed transitions, and also exclude $M2$ multipolarity for the strongest lines. The $M2$ multipolarity cannot be excluded for the weak 795.7-keV line, although this assignment is unlikely. If this transition is $M2$, it would be the fastest one in this mass region.

β-transition rates can provide independent limits on spins and parities. The strong β^- transitions from the 0^+ g.s. in ^{132}Sn to the 1325.2- and 2268.3-keV states in ^{132}Sb with logft values of 4.01(5) and 4.80(9), respectively, firmly imply spin/parity $I^\pi = 1^+$ for those levels [2–4]. The 1325.2-keV state decays to the g.s. via two transition cascades, each including one (firmly assigned) $M1$ transition and another one which is either $M1$, $E2$, or $M1 + E2$. Thus I^π(g.s.) must take any integer value between 0^+ and 4^+. This choice is further limited to 3^+ or 4^+ by a fast allowed β transition [logft=5.83(8)] from the g.s. of ^{132}Sb to the 4^+ state in ^{132}Te [20]. These two choices, however, are not equally probable. The pattern of the ^{132}Sb$\rightarrow$^{132}Te β decay clearly favors the $I^\pi = 4^+$ assignment for the parent state since no β feeding to the 2_1^+ state is observed, while there is a strong indirect γ feeding (from the higher-lying levels directly β fed) to the 6_1^+ level.

The angular correlation results are listed in Table III for two individual cases: I^π(g.s.)=4^+ and 3^+. All strong transitions were considered to be either $E1$, $M1$, $E2$, or mixed $M1/E2$, unless limited further by the results quoted above. Meaningful correlations were obtained for nine transition pairs that are labeled in Table III column 2 by the energies of the γ-ray pair, E_1-E_2, in the order they appear in a cascade. For a given cascade an angular correlation function was fitted with fixed spins listed in column 3. During the fit, one of the δ parameters was allowed to vary while the other δ was kept fixed, either at δ=0 as in the case of a $E1$ or a stretched $E2$ transition, or restricted to a value determined earlier and given in column four. The result of the χ^2 fit, i.e., the value of the varied δ parameter determined at $\chi^2_{\min}$, is listed in column 5. Due to the long lifetime of the 85.6-keV state ($T_{1/2} \approx 16$ ns), there may be additional systematical errors due to attenuation of the angular correlations that involve the 85.6-keV transition.

A. Case: I^π(g.s.)=4^+

In this case, spins and parities of the 1078.3-, 529.1-, and 85.6-keV levels are assigned as 2^+, $3^\pm$, and 3^+, respectively, based on the cascades of two transitions connecting the 1^+ state at 1325.2-keV and the 4^+ g.s. Since each cascade must carry three units of angular momentum via one transition which is known to be of dipole character, and another one which can be at the most a quadrupole (higher multipolarities are excluded), it must consist of a stretched dipole and a stretched quadrupole transitions giving a unique spin determination of the intermediate level. In particular, the 247-1078 γ cascade, where the 246.9-keV transition is a stretched $M1$, and thus the 1078.3-keV transition must be a stretched $E2$, defines I^π=2^+ for the 1078.3-keV state. Similarly, $I^\pi = 3^+$ is defined for the 85.6-keV level by the strong 1240-86 cascade, in which the 85.6-keV line is a stretched $M1$, and the 1239.6-keV transition must be a stretched $E2$. The 796-529 cascade defines spin $I = 3$ for the 529.1-keV state. In this case the 529.1-keV γ ray is either a stretched $E1$ or $M1$, while the 795.7-keV line is either a stretched $E2$ (the most likely choice) or $M2$ (less likely, but cannot be excluded at present). The parity of the level is either positive or negative.

The spin of the 426.1-keV level is uniquely defined as 2^+. Although the 340.5-keV line, which is predominantly $M1$, defines I^π=2^+, 3^+, or 4^+ for the 426.1-keV state, yet the 4^+ alternative is ruled out since the strong 899.0-keV transition from the 1^+ state to this level is not $M3$. Furthermore, the 3^+ choice is excluded by the angular distribution results for the 899-340 cascade, since the $\chi^2_{\min}$ for the 1^+–3^+–3^+ spin sequence (here the 899-keV transition must be a stretched $E2$) is much higher than for the alternative spin sequence.

With a unique spin determination of 2^+ (1078.3), $3^\pm$ (529.1), 2^+ (426.1), and 3^+ (85.6) for the intermediate levels between the 1^+ state at 1325.2 keV and the 4^+ g.s., one can use the $\gamma\gamma(\theta)$ results to obtain $\delta(E2/M1)$ mixing ratios for the involved transitions. In the first step, see Table III, data entries #2–10, we determine δ_{247} from the 247-1078 cascade and use it to obtain δ for the 652.3-, 549.2-, and 992.7-keV lines. Then we use these newly determined δ values to obtain the mixing ratio for the 529.1- and 85.6-keV lines. From the 1240-86 cascade we get an independent estimate of δ_{86} which compares closely with the value deduced from the 993-86 cascade. In the analysis of the 340-86 cascade we use the average δ_{86} to deduce δ_{340}. Note that the fitted value of δ_{340} is not precise. We combine this δ_{340} with the limit deduced from the lifetime result to yield $-0.20 \leq \delta_{340} \leq 0$, which was used in the subsequent analysis of the 899-340 cascade (see Fig. 3).

Only positive parity ($I^\pi = 3^+$) was considered for the 529.1-keV state. If the parity of this state is negative ($I^\pi = 3^-$), then both the 549.2- and 529.1-keV transitions would be $E1$ with $\delta(M2/E1) \sim 0$. This situation cannot be resolved by the present data.

B. Case: I^π(g.s.)=3^+

From arguments similar to those given above one obtains the following spin assignments for the intermediate levels: I^π=2^+ for the 1078.3-keV state, $2^\pm$ or $3^\pm$ for the 529.1-keV level, 2^+ or 3^+ for the 426.1-keV state, and

TABLE III. Angular correlation results for ^{132}Sb. See text for discussion.

#	E_1-E_2 [a] (keV)	$I_1 \xrightarrow{\delta_1} I_2 \xrightarrow{\delta_2} I_3$ ($\hbar$)	Restricted or fixed δ	Minimum in varied δ
			Results assuming I^π(g.s.)=4^+	
1	899–340	1^+–3^+–3^+	$\delta_1 = \delta_{899}(M3/E2)$=0 [b]	none in $\delta_2 = \delta_{340}$ [c]
2	247–1078	1^+–2^+–4^+	$\delta_2 = \delta_{1078}(M3/E2)$=0 [b]	δ_1=δ_{247}=−0.14(6)
3	247–652	1^+–2^+–2^+	$\delta_1 = \delta_{247}$=−0.14(6)	δ_2=δ_{652}=−0.7(6)
4	247–549	1^+–2^+–3^+	$\delta_1 = \delta_{247}$=−0.14(6)	δ_2=δ_{549}=−0.07(21)
5	549–529	2^+–3^+–4^+	$\delta_1 = \delta_{549}$=−0.07(21)	δ_2=δ_{529}=−0.23(23)
6	247–993	1^+–2^+–3^+	$\delta_1 = \delta_{247}$=−0.14(6)	δ_2=δ_{993}=−0.49(8)
7	993–86	2^+–3^+–4^+	$\delta_1 = \delta_{993}$=−0.49(8)	δ_2=δ_{86}=−0.09(2)
8	1240-86	1^+–3^+–4^+	$\delta_1 = \delta_{1240}(M3/E2)$=0 [b]	δ_2=δ_{86}=−0.10(2)
9	340–86	2^+–3^+–4^+	$\delta_2 = \delta_{86}$=−0.095(14) [d]	δ_1=$\delta_{340}\leq$0
10	899–340	1^+–2^+–3^+	$-0.20\leq \delta_2 = \delta_{340} \leq 0$	δ_1=δ_{899}=−0.22(10)
			Results assuming I^π(g.s.)=3^+	
11	247–993	1^+–1^+–2^+	$\mid\delta_1\mid$=$\mid\delta_{247}\mid\leq$0.20	none in $\delta_2 = \delta_{993}$ [c]
12	899–340	1^+–3^+–3^+	$\delta_1 = \delta_{899}(M3/E2)$=0 [b]	none in $\delta_2 = \delta_{340}$ [c]
13	1240–86	1^+–3^+–3^+	$\delta_1 = \delta_{1240}(M3/E2)$=0 [b]	none in $\delta_2 = \delta_{86}$ [e]
14	247–993	1^+–2^+–2^+	$\mid\delta_1\mid$=$\mid\delta_{247}\mid\leq$0.20	δ_2=$\delta_{993} = -0.23^{+0.10}_{-0.05}$
15	247-1078	1^+–2^+–3^+	$\mid\delta_1\mid$=$\mid\delta_{247}\mid\leq$0.20	δ_2=$\delta_{1078} = -0.14^{+0.04}_{-0.15}$
16	247–652	1^+–2^+–2^+	$\mid\delta_1\mid$=$\mid\delta_{247}\mid\leq$0.20	δ_2=δ^A_{652}=$0.09^{+0.50}_{-0.06}$
17		1^+–2^+–3^+	$\mid\delta_1\mid$=$\mid\delta_{247}\mid\leq$0.20	δ_2=δ^B_{652}=−0.70(24)
18	899–340	1^+–2^+–2^+	$\mid\delta_2\mid$=$\mid\delta_{340}\mid\leq$0.20	δ_1=$\delta^A_{899} = -0.20(2)$
19		1^+–3^+–2^+	$\delta_1 = \delta^B_{899}$=0	δ_2=δ^B_{340} =0.18(1)
20	340–86	2^+–2^+–3^+	$\mid\delta_1\mid$=$\mid\delta_{340}\mid\leq$0.20	$\delta^A_{86} = -0.06^{+0.04}_{-0.02}$
21		3^+–2^+–3^+	$\delta_1 = \delta^B_{340}$ =0.18(1)	δ^B_{86} =0.03(4)
22	993-86	2^+–2^+–3^+	$\delta_2 = \delta^A_{86} = -0.06^{+0.04}_{-0.02}$	$\delta_1 = \delta^A_{993}$=0.32(19)
23			$\delta_2 = \delta^B_{86}$ =0.03(4)	$\delta_1 = \delta^B_{993}$=0.32(6)
24	1240-86	1^+–2^+–3^+	$\delta_2 = \delta^A_{86} = -0.06^{+0.04}_{-0.02}$	$\delta_1 = \delta^A_{1240}$=$-0.4^{+0.2}_{-0.6}$
25			$\delta_2 = \delta^B_{86}$ =0.03(4)	$\delta_1 = \delta^B_{1240}$=−0.26(5)
26	247–549	1^+–2^+–2^-	$\delta_2 = \delta_{549}(M2/E1)$=0 [f]	δ_1=δ^C_{247}=−0.30(11)
27		1^+–2^+–3^-	$\delta_2 = \delta_{549}(M2/E1)$=0 [f]	δ_1=δ^D_{247}=−0.2(4)
28		1^+–2^+–2^+	$\mid\delta_1\mid$=$\mid\delta_{247}\mid\leq$0.20	δ_2=δ^E_{549}=$-0.4^{+0.3}_{-0.7}$
29		1^+–2^+–3^+	$\mid\delta_1\mid$=$\mid\delta_{247}\mid\leq$0.20	δ_2=δ^F_{549}=$-0.1^{+0.3}_{-0.5}$
30	549–529	2^+–2^-–3^+	$\delta_{1,2} = \delta_{549}(M2/E1)$=$\delta_{529}(M2/E1)$=0 [f]	[g]
31		2^+–2^+–3^+	$\delta_1 = \delta^E_{549}$=$-0.4^{+0.3}_{-0.7}$	δ_2=δ^E_{529}=−0.05(11)
32	549–529	2^+–3^-–3^+	$\delta_{1,2} = \delta_{549}(M2/E1)$=$\delta_{529}(M2/E1)$=0 [f]	[g]
33		2^+–3^+–3^+	$\delta_1 = \delta^F_{549}$=$-0.1^{+0.3}_{-0.5}$	δ_2=δ^F_{529}=$-0.4^{+0.2}_{-0.3}$

[a] Transition E_2 follows transition E_1 in a cascade. Note, that results in this table were averaged over two independent data sets — one for E_1-E_2 and second for its reciprocal: E_2-E_1.

[b] Assumed a stretched $E2$ transition.

[c] $\chi^2 \geq 3\chi^2_{\rm min}$ for this combination. In the case of I^π(g.s.)=4^+ and I^π=3^+ for the 85.6-keV level, the choice of I^π=3^+ is rejected for the intermediate state at 426.1 keV, that is deexcited by the 340.5-keV transition.

[d] An average of the results in row #7 and #8.

[e] $\chi^2 \geq 5\chi^2_{\rm min}$ for this combination. Choice of I^π=3^+ is thus rejected for the intermediate level at 85.6 keV, that is deexcited by the 85.6-keV transition.

[f] Assumed a pure $E1$ transition.

[g] $\chi^2_{\rm min}$ for this fit is similar to $\chi^2_{\rm min}$ for other spin/parity combinations for this cascade.

I^π= 2^+ for the 85.6-keV level. The assignment of spin 1^+ for the 1078.3- and 426.1-keV states is rejected due to a lack of observed β feeding to those states. Also, the angular correlation for the 247-993 cascade (entry #11) rules out spin 1^+ for the 1078.3-keV state, while the results for the 1240-86 cascade (entry #13) rule out spin 3^+ for the 85.6-keV level.

Since there are two choices of spin for each of the 426.1- and 529.1-keV states, there are multiple entries in Table III. Those marked by "A" and "B" refer to the $\delta(E2/M1)$ mixing ratios deduced assuming spin 2^+ and 3^+ for the 426.1-keV state, respectively, while the $\delta(E2/M1)$ mixing ratios "C," "D," "E," and "F" refer to spins 2^-, 3^-, 2^+, and 3^+, respectively, for the 529.1-keV state.

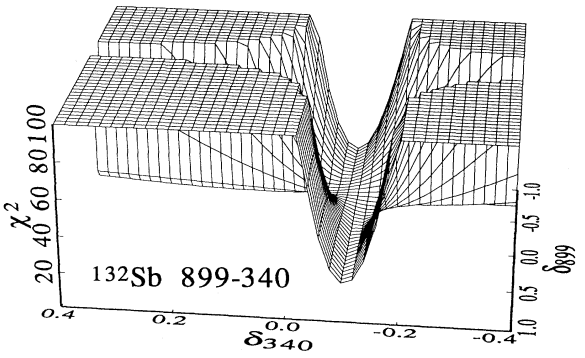

FIG. 3. A χ^2 surface for the 899-340 transition pair and the $1^+ \xrightarrow{\delta_{899}} 2^+ \xrightarrow{\delta_{340}} 3^+$ spin sequence obtained in the $\gamma\gamma(\theta)$ measurement. Note, that both $\delta(E2/M1)$ are allowed to vary giving a three-dimensional χ^2 surface.

C. Additional case: I^π(g.s.)=3$^-$

If we neglect the conversion coefficient result for the 899.0-keV line and rely on other evidence combined with the $\gamma\gamma(\theta)$ results we can provide independent evidence against the negative parity assignment for the g.s. of ^{132}Sb. Note that according to the recent compilation of logft values by Didierjean and Walter [21] (who updated the compilation by Raman and Gove [22]) the fast logft value for the g.s. decay of ^{132}Sb does not exclude this transition to be first forbidden since such fast transitions are observed in close vicinity to the doubly magic nuclei.

Spin I^π=3$^-$ is the only negative parity choice which satisfies the requirements of the conversion coefficient (excluding the 899.0-keV line), level lifetime, and logft measurements. We have examined the angular correlation data for all possible (and related) spin combinations and obtained a few independent estimates of $\delta(E2/M1)$ for the intense 85.6-, 246.9-, and 340.5-keV lines (this was possible since most γ cascades included an $E1$ transition for which δ is restricted). A few of these independent estimates were found several standard deviations apart which prove that the spin/parity I^π(g.s.)= 3$^-$ is not compatible with the angular distribution data.

IV. TRANSITION RATES IN ^{132}Sb

Although I^π(g.s.)= 3$^+$ cannot be rigorously ruled out at present, the 4$^+$ alternative is clearly favored by the experimental evidence and model considerations. Our present results illustrated in Fig. 1 are in a full agreement with those obtained previously [2,3] while providing important clarification of the earlier assignments.

The earlier works extensively used simple shell model calculations to interpret the experimental results. One observes a remarkable agreement between the configuration assignments of Kerek *et al.* [2] and Stone, Faller, and Walters [3] based on simple shell model considerations, and the sophisticated calculations by Erokhina and Isakov [5] that are used in the present work. In particular the following particle-hole configurations were found as dominant components in the wave functions of the observed states: $\pi g_{7/2}\nu d_{3/2}^{-1}$ in the g.s., and levels at 85.6 and 426.1 keV, $\pi g_{7/2}\nu s_{1/2}^{-1}$ in the 529.1-keV state, $\pi d_{5/2}\nu d_{3/2}^{-1}$ in the levels at 1078.3 and 1325.2 keV, and $\pi g_{7/2}\nu d_{5/2}^{-1}$ in the 2268.3-keV level. While the earlier configuration assignments were based on excitation energies, energy splittings within multiplets, and logft values, the present work extends this synonymous comparison to include for the first time the theoretical and experimental results for a large number of transition rates in ^{132}Sb.

The calculations were performed in the framework of the theoretical approach presented in [5] taking into account the configuration mixing and ground state correlations. The method of Green functions used by us is, in its essence, equivalent to the quasiboson approximation, and has also been used in the calculations of even-even nuclei with two particles or holes above ^{132}Sn [23]. We have used a single-particle basis which contained all states in the intervals $28 < Z < 82$ and $50 < N < 126$. The configuration splitting and configuration mixing were accomplished via a finite range effective interaction which contained spin, isospin, and tensor components. All the parameters of the theory were defined earlier from calculations of nuclei close to ^{208}Pb and ^{146}Gd [24,25].

With the exception of the $B(M1)$ rate for the 85.6-keV line measured by Kerek *et al.* [2], no $B(M1)$ or $B(E2)$ transition rates were known up to now. However, it was possible to demonstrate [2] that the experimental value of $B(M1) = 0.0022(3)\mu_N^2$ closely agrees with a predicted rate for the $M1$ transition between the 3$^+$ and 4$^+$ members of the same proton-neutron multiplet if the configuration involved is $\pi g_{7/2}\nu d_{3/2}^{-1}$, but not if it is $\pi g_{7/2}\nu s_{1/2}^{-1}$ or $\pi d_{5/2}\nu d_{3/2}^{-1}$. The $B(E2)$ predictions of 43, 24, and 12 e^2 fm^4 were also made for those cases, respectively, but the earlier experimental results of $B(E2)$ <164 e^2 fm^4 [2] was not precise enough to allow any conclusion. The new result of 36(11) e^2 fm^4 (see Table IV) is in close agreement with the predicted value of 43 e^2 fm^2 for the $\pi g_{7/2}\nu d_{3/2}^{-1}$ configuration [2]. The situation is, however, considerably more complex as shown by the new experimental and theoretical results. Our calculations revealed that the eigenvectors of low-lying states in ^{132}Sb have distinct leading components with amplitudes of the order of 0.7–0.9 and thus may only be approximately classified in terms of proton particle-neutron hole multiplets.

Table IV provides a comparison of the experimental results and model predictions for the $\delta(E2/M1)$ mixing ratios as well as the $B(M1)$ and $B(E2)$ rates. In particular, the transitions from the 426.1-keV level, which take place within the $\pi g_{7/2}\nu d_{3/2}^{-1}$ configuration, are well described by the theory. Less trivial is the good agreement for the transitions deexciting the 529.1 (3_2^+) and 1078.3 (2_2^+) levels, which all represent off-diagonal matrix elements. In the first case we have transitions of the type $\pi g_{7/2}\nu s_{1/2}^{-1} \rightarrow \pi g_{7/2}\nu d_{3/2}^{-1}$, while in the second case they are of the type $\pi d_{5/2}\nu d_{3/2}^{-1} \rightarrow \pi g_{7/2}\nu d_{3/2}^{-1}$

TABLE IV. Experimental transition rates in ^{132}Sb; comparison with theoretical predictions [5].

Level [a] (keV)	E_γ (keV)	γ Branching	$\delta(E2/M1)$ [b]	$\delta(E2/M1)^{\rm th}$	$B(M1)^{\rm exp}$ ($\times10^{-3}$ μ_N^2)	$B(M1)^{\rm th}$ ($\times10^{-3}$ μ_N^2)	$B(E2)^{\rm exp}$ (e^2 fm^4)	$B(E2)^{\rm th}$ (e^2 fm^4)
85.6	85.6	0.506 [c]	−0.095(14)	−0.081	2.02(3)	7.0	36(11)	90
426.1	340.5	0.977 [c]	$-0.20\leq\delta\leq0$	−0.057	61(7)	28	76(76)	11
	426.1	$\leq$0.01	[d]				<26	3.7
529.1	103.0			+0.054		3.7		14
	443.5	0.097		−0.049	>3.4 [e]	40		7.0
	529.1	0.903	−0.23(23)	+0.013	>17.5	141		1.2
1078.3	549.2	0.052	−0.07(21)	−0.099	4.8(26)	1.8	$1.1^{+15.4}_{-1.1}$	0.84
	652.3	0.061	−0.7(6)	−0.70	2.2(17)	0.30	37(30)	4.9
	992.7	0.831	−0.49(8)	−0.38	10(5)	3.4	36(23)	7.3
	1078.3	0.056	[d]				8.4(45)	6.5
1325.2	246.9	0.424 [c]	−0.14(6)	−0.019	>29	746	>45	61
	795.7	0.0031	[d]				>0.15	1.4
	899.0	0.449	−0.22(10)	−0.20	>0.66	10.8	>0.17	7.4
	1239.6	0.098	[d]				>0.51	12
2268.3	943.1			−0.53		6.7		30
				(−0.31)		(100)		(153)
	1190.0			−0.29		27		23
				(−2.3)		(2.5)		(127)
	1739.1	0.148	[d]				>0.09	61
								(37)
	1842.2	0.852		−0.026	>0.09 [e]	103		0.29
				(0.42)		(6.5)		(4.9)
	2182.7		[d]					0.10
								(0.78)

[a] $T_{1/2}$ were taken from Table II.
[b] From Table III for the case I^π(g.s.)=4^+.
[c] $\alpha_{\rm tot}$=0.974, 0.062, and 0.024 for the 85.6-, 246.9-, and 340.5-keV transitions, respectively (from Ref. [4]).
[d] $M1$ is not allowed by the spin selection rules; $\delta(M3/E2)=0$.
[e] $\delta(E2/M1)$ has not been determined; assumed dominance of $M1$.

(and $\pi d_{5/2}\nu d_{3/2}^{-1}\rightarrow\pi g_{7/2}\nu s_{1/2}^{-1}$ for the transition to the 529.1-keV level). In the cases mentioned above we have single-particle transformations of the $\nu s_{1/2}\rightarrow\nu d_{3/2}$ or $\pi d_{5/2}\rightarrow\pi g_{7/2}$ types. Such transitions are forbidden for $M1$-radiation in a model not accounting for configuration mixing. Thus a close agreement with the experiment both for the $B(E2,M1)$ and $\delta(E2/M1)$ values confirms the validity of our model. Of special interest is the $2_2^+\rightarrow3_2^+$ transition to the 529.1-keV level. Here we have simultaneous proton and neutron transformations $\pi d_{5/2}\rightarrow\pi g_{7/2}$ and $\nu d_{3/2}\rightarrow\nu s_{1/2}$, respectively. Without configuration mixing this transition is forbidden both for $M1$ and $E2$ radiations. Configuration mixing "opens" this transition, though its transition probabilities for the $M1$ and $E2$ radiations remain small. The agreement with the experiment, which is demonstrated in this work, is the most impressive confirmation of the theoretical scheme and the effective forces used in the calculations.

Our model predicts existence of three low-lying 1^+ states at the excitation energies equal to ~1.5, 2.1, and 2.4 MeV and having the dominant configurations of $\pi d_{5/2}\nu d_{3/2}^{-1}$, $\pi g_{7/2}\nu d_{5/2}^{-1}$, and $\pi s_{1/2}\nu d_{3/2}^{-1}$, respectively. The first state may be populated in the spin-flip β^- decay of ^{132}Sn and corresponds to the 1325.2-keV level in ^{132}Sb populated with log$ft\sim4.0$. As seen in Table IV, this picture also agrees with the electromagnetic decay properties of this level. The Gamow-Teller β^- transitions to the other predicted levels may take place only due to admixtures of the $\pi d_{5/2}\nu d_{3/2}^{-1}$, $\pi s_{1/2}\nu s_{1/2}^{-1}$,... components, having the same n and l quantum numbers for both protons and neutrons, and must therefore be retarded. The 2268.3-keV level populated with log$ft\sim5.0$ is thus one of these two levels. We adopt this state as the 1_2^+ model state with a dominant configuration of $\pi g_{7/2}\nu d_{5/2}^{-1}$. The theoretical predictions for the case that the 2268.3-keV level is the 1_3^+ theoretical state are given in Table IV in brackets. Neither of the assignments contradict the experimental $B(E2,M1)$ rates, but the branching ratios from the 2268.3-keV level are better reproduced if it has a dominant $\pi g_{7/2}\nu d_{5/2}^{-1}$ configuration.

V. CONCLUSIONS

The structure of ^{132}Sb has been investigated via the measurements of conversion electron, $\gamma\gamma(\theta)$ angular correlations, and fast timing $\beta\gamma\gamma(t)$ coincidences. Spin and parity assignments were made to the low-lying states in ^{132}Sb largely confirming the tentative assignments given

before. We have determined eight $\delta(E2/M1)$ mixing ratios, and several $B(M1)$ and $B(E2)$ transition rates which have allowed for the first time a critical verification of the model predictions by Erokhina and Isakov [5].

The present work has revealed that the properties of the neutron-rich nucleus ^{132}Sb having a proton particle-neutron hole pair above the doubly magic ^{132}Sn may be described on the same grounds as that of the ^{208}Bi nucleus adjacent to the ^{208}Pb core. Our study has thus established that the classical shell numbers and the effective interaction remain unchanged for nuclei in this region as compared to those near the stability line. An excellent agreement between experiment and the model predictions is noticed which manifests the adequacy of the theory employed.

ACKNOWLEDGMENTS

We thank Leif Jacobsson for the preparation of the targets, ion sources and a smooth operation of the OSIRIS separator that make our measurements possible. This work was supported in part by the Swedish Natural Science Research Council.

[1] B. Fogelberg, M. Hellström, L. Jacobsson, D. Jerrestam, L. Spanier, and G. Rudstam, Nucl. Instrum. Methods Phys. Res. Sect. B **70**, 137 (1992).
[2] A. Kerek, G. B. Holm, P. Carlé, and J. McDonald, Nucl. Phys. **A195**, 159 (1972).
[3] C. A. Stone, S. H. Faller, and W. B. Walters, Phys. Rev. C **39**, 1963 (1989).
[4] Yu. V. Sergeenkov, Nucl. Data Sheets **65**, 277 (1992).
[5] K. I. Erokhina and V. I. Isakov, Phys. At. Nucl. **57**, 198 (1994).
[6] L. Jacobsson, B. Fogelberg, B. Ekström, and G. Rudstam, Nucl. Instrum. Methods Phys. Res. Sect. B **26**, 223 (1986), and references therein.
[7] F. Rösel, H. M. Fries, K. Alder, and H. C. Pauli, At. Data Nucl. Data Tables **21**, 92 (1978).
[8] H. Mach, R. L. Gill, and M. Moszyński, Nucl. Instrum. Methods Phys. Res. Sect. A **280**, 49 (1989).
[9] R. G. Clark, L. E. Glendenin, and W. L. Talbert, in *Proceedings of the Symposium on the Physics and Chemistry of Fission*, Rochester, 1973 (IAEA, Vienna, 1974), Vol. 2, p. 221.
[10] M. Moszyński and H. Mach, Nucl. Instrum. Methods Phys. Res. Sect. A **277**, 407 (1989).
[11] H. Mach, F. K. Wohn, G. Molnár, K. Sistemich, John C. Hill, M. Moszyński, R. L. Gill, W. Krips, and D. S. Brenner, Nucl. Phys. **A523**, 197 (1991).
[12] H. Mach, M. Moszyński, and R. L. Gill (unpublished).
[13] H. Mach, W. Nazarewicz, D. Kusnezov, M. Moszyński, B. Fogelberg, M. Hellström, L. Spanier, R. L. Gill, R. F. Casten, and A. Wolf, Phys. Rev. C **41**, R2469 (1990).
[14] H. Mach, F. K. Wohn, M. Moszyński, R. L. Gill, and R. F. Casten, Phys. Rev. C **41**, 1141 (1990).
[15] B. Fogelberg, M. Hellström, D. Jerrestam, A. Kerek, H. Mach, L. O. Norlin, J. P. Omtvedt, and H. Prade, in *Proceedings of the 6th International Conference on Nuclei Far From Stability and 9th International Conference on Atomic Masses and Fundamental Constants*, Bernkastel-Kues, 1992, edited by R. Neugart and A. Wöhr, IOP Conf. Proc. No. 132 (Institute of Physics and Physical Society, London, 1993), p. 569.
[16] H. Mach, B. Fogelberg, M. Hellström, D. Jerrestam, A. Kerek, L. O. Norlin, and J. P. Omtvedt, in *Proceedings of the 8th International Symposium on Capture Gamma-ray Spectroscopy and Related Topics*, Fribourg, 1993, edited by J. Kern (World Scientific, Singapore, 1994), p. 407.
[17] D. C. Camp and A. L. Van Lehn, Nucl. Instrum. Methods **76**, 192 (1969).
[18] T. Yamazaki, At. Data Nucl. Data Tables **A3**, 1 (1967).
[19] K. S. Krane, R. M. Steffen, and R. M. Wheeler, At. Data Nucl. Data Tables **A11**, 5 (1973).
[20] A. Kerek, P. Carlé, and S. Borg, Nucl. Phys. **A224**, 367 (1974).
[21] F. Didierjean and G. Walter, Centre de Recherches Nucléaires, IN2P3 et Université Louis Pasteur, Report No. CRN 94-01 (unpublished).
[22] S. Raman and N. B. Gove, Phys. Rev. C **7**, 1995 (1973).
[23] K. I. Erokhina and V. I. Isakov, Izv. Russ. Akad. Nauk Ser. Fiz. **56**, 78 (1992) [Bull. Russ. Acad. Sci. Phys. **56**, 1720 (1992)].
[24] V. I. Isakov, S. A. Artamonov, and L. A. Sliv, Izv. Russ. Akad. Nauk Ser. Fiz. **41**, 2074 (1977) [Bull. Russ. Acad. Sci. Phys. **41**(10), 72 (1977)].
[25] S. A. Artamonov, V. I. Isakov, and I. A. Lomachenkov, Yad. Fiz. **45**, 33 (1987) [Sov. J. Nucl. Phys. **45**, 20 (1987)].